Langevin simulations of stripe forming systems with long-range isotropic competing interactions

2016 J. Phys.: Conf. Ser. 686 012005

(http://iopscience.iop.org/1742-6596/686/1/012005)

Langevin simulations of stripe forming systems with long-range isotropic competing interactions

Lucas Nicolao

Departamento de Física, Universidade Federal de Santa Catarina, 88040-970, Florianópolis, Brazil.

E-mail: lucas.nicolao@ufsc.br

Alejandro Mendoza-Coto

Departamento de Física, Universidade Federal do Rio Grande do Sul, Caixa Postal 15051, 91501-970, Porto Alegre, Brazil.

Daniel A. Stariolo

Departamento de Física, Universidade Federal Fluminense and National Institute of Science and Technology for Complex Systems, 24210-346, Niterói, Brazil.

Abstract.

We address the critical properties of the isotropic-nematic phase transition in stripe forming systems. We focus on isotropic models in which a short range attractive interaction competes with a long range repulsive interaction decaying as a power-law, paying particular attention to the cases in which this interaction is of dipolar or Coulomb types. Using Langevin dynamics simulations we show that these models belong to different universality classes. The numerical algorithms developed for each case are presented and discussed in detail. The obtained results are in agreement with recent theoretical predictions [1], according to which the orientational transition belongs to the Kosterlitz-Thouless universality class for dipolar systems, while it is of the second-order type for Coulomb systems.

1. Introduction

Competing interactions usually lead to heterogeneities in the local order parameter in the form of completely disordered patterns as present, e.g. in spin glasses [2], or formation of patterns or domains as observed in many systems like magnetic thin films [3], diblock copolymers [4], and quasi two dimensional electronic quantum liquids [5]. The identification and characterisation of ordered phases in these systems is not straightforward because of the spatially heterogeneous nature of the order parameter (see Figure 1 for an experimental example). Broken translation and rotation symmetry in space are usually associated with phase transitions. Early theoretical descriptions of phase transitions in these systems exploited an analogy with liquid crystals, systems of more or less rigid rod-like molecules which can order in a large variety of phases with broken translation or rotation symmetry. Like in liquid crystals, where orientation of the axes

of the molecules are described by a vector called "director", in pattern forming systems like ultrathin magnetic films a director can be associated to the direction of interfaces or domain walls and are useful to identify orientational order of the patterns (see Figure 2).

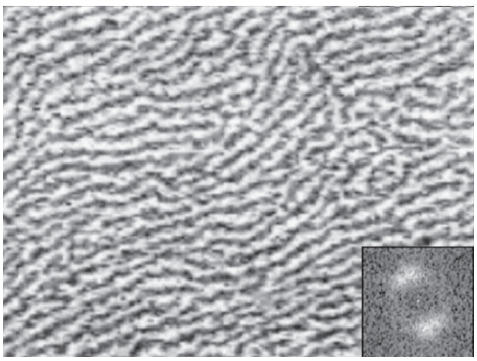

Figure 1. Stripe domains of magnetization in ultrathin magnetic films of 2.6 ± 0.6 AL thick fcc Fe on Cu(100), as imaged by scanning electron microscopy with polarisation analysis (SEMPA). This image's horizontal dimension is ≃ 24 μm. Inset: Fourier power spectrum. Adapted from [6].

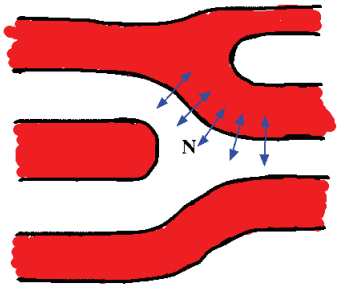

Figure 2. Schematic representation of a striped pattern with local orientation of interfaces characterised by the director vector.

In a pioneering work in the seventies S. A. Brazovskii showed that some antiferromagnets with nearly isotropic competing interactions acting at different scales suffer an instability leading to anisotropic low temperature phases with modulation of the local order parameter in the form of charge or spin density waves [7]. The instability occurs at a characteristic non zero wave vector k_0 leading precisely to modulated structures in the charge density or magnetization. This kind of instability was realised to be of much more general applicability and soon after Brazovskii's work J. Swift and P. C. Hohenberg proposed a similar mechanism to explain the convective instability manifested by the appearance of rolls in the Rayleigh-Bénard convection [8]. Motivated by the recent discovery of high temperature superconductivity, V. J. Emery and S. A. Kivelson introduced in the early nineties a model with competition between a kinetic term and the long-range Coulomb interaction between electrons which leads also to phase separation in the charge density and the appearance of modulated order in the form of stripes[9]. In the following years experiments on high T_c superconductors, doped Mott insulators and quantum Hall systems established the presence of anisotropies in transport properties, and new states of matter at ultra low temperatures, the so called "electronic liquid crystals", were proposed to explain the observations [10, 11, 12]. Since then, the presence of stripe, nematic or hexatic order in the charge and/or spin degrees of freedom of quasi two dimensional strongly correlated electronic systems has been firmly established as part of the phenomenology around high T_c superconductivity, although its relevance to the appearance of superconducting properties is still a matter of debate [13, 14].

Despite the large amount of experimental and theoretical work done on different systems showing modulated order, still there are many properties of the phase diagrams and phase transitions which are not known. In particular, the characterisation of the nature of different phases and the critical properties have been shown to be subtle. Experiments able to probe the critical properties of phase transitions in these systems have still to be designed and

executed, while theoretical approaches suffer from some well known but severe limitations in their predictability. First of all, the nearly two dimensional nature of the systems makes the precise characterisation of their critical properties a subtle task. It is known that two dimensions is near the lower critical dimension of many systems and the fluctuation effects are rather strong [15], making predictions from naive mean field approximations or simulations of moderately small system sizes unreliable. Furthermore, the very nature of the *nematic phases*, phases with orientational but not translational order, leads to an order parameter which measures anisotropies in nearest-neighbour correlation functions, i.e. the order parameter is a two-point function in space, and then simple mean field theories are unable to capture the presence of a nematic phase.

Another important issue that hinders the full description of phase diagrams is the fact that the relevant scales can vary many orders of magnitude by tuning an external parameter and that is true even far from critical points. In general the modulation length of stripes or orientationally ordered states depends on external parameters like temperature and magnetic fields, but mainly on the relative strength of the competing interactions. In this way, the modulation length can range from a few interatomic or lattice spacings up to hundreds or thousands of them. Examples of systems in which the relevant physics corresponds to one or the other extreme can be found [16]. Clearly, the critical properties in both cases can be very different, anisotropies induced by the lattice structure are relevant when the modulation length is of the order of the lattice spacing, but probably not relevant for modulations spanning thousands of lattice spacings. This multiscale phenomenology strongly complicates the modelling and simulation of stripe forming systems.

Here we address the critical properties of stripe forming systems with isotropic long-range competing interactions with variable range [1]. We give special attention to the high temperature phase transition between an isotropic and nematic phases, and the relevance of the range of the interaction to the nature of this rotational symmetry breaking transition. In the next section we motivate our general mesoscopic approach to the two pertinent stripe forming systems, with Coulomb or dipolar interactions, discussing general issues about the nematic phases in these systems. We also review a recently developed elastic theory that accounts for the correct effect of long-range interactions, predicting distinct behaviour for the two cases. Later we present the technical details involved in performing Langevin simulations of these models. We finish presenting preliminary results confirming these predictions, and discussing future directions.

2. Coarse-grained model and elastic theory

The long wavelength limit, in which the modulation spans thousands of electrons or spins, is particularly relevant in two well known physical systems: ultrathin magnetic films [6, 17, 18] and two dimensional electronic liquids [10, 19, 20, 21]. In the first case, stripes or orientated patterns emerge from the competition between the short range exchange interaction and the long-range dipolar interaction. In the second case, the nature of the competition is more subtle coming from the competition between the kinetic (quantum dynamics) term and the long-range Coulomb interaction. In this limit, both cases can be modelled by an effective coarse-grained Hamiltonian in two dimensions of the form:

$$\mathcal{H}[\phi(\vec{x})] = \frac{1}{2}\int d^2x\ \left(\vec{\nabla}\phi(\vec{x})\right)^2 + \frac{1}{2}\int d^2x \int d^2x'\ \phi(\vec{x})J(\vec{x}-\vec{x'})\phi(\vec{x'}) + \frac{1}{2\beta}\int d^2x\ V(\phi(\vec{x})) \quad (1)$$

where $\beta = 1/k_BT$ and $V(\phi) = -\frac{r}{2}\phi^2 + \frac{1}{12}\phi^4$ is a local potential. The first term can be seen as the continuous limit of a nearest-neighbour interaction while the second, competing term, has the form $J(\vec{x}) = J/x^\alpha$, which allows to analyse in a unified way short range (large α) and long-range (small α) interactions. Physically relevant examples are the Coulomb interaction

($\alpha = 1$) and the dipolar interaction between out of plane magnetic moments ($\alpha = 3$). Note that this effective Hamiltonian has strictly isotropic interactions and the anisotropic phases, like the nematic one, can only emerge from the spontaneous breaking of the rotational symmetry in real space. In fact, working with a similar Hamiltonian, D. G. Barci and D. A. Stariolo [22] showed that the rotational symmetry of the characteristic wave vector $\vec{k}_0$ present at relatively high temperatures is spontaneously broken at a critical temperature T_c leading to a isotropic-nematic phase transition. Nematic order in this case means that the stripes possess an orientational order

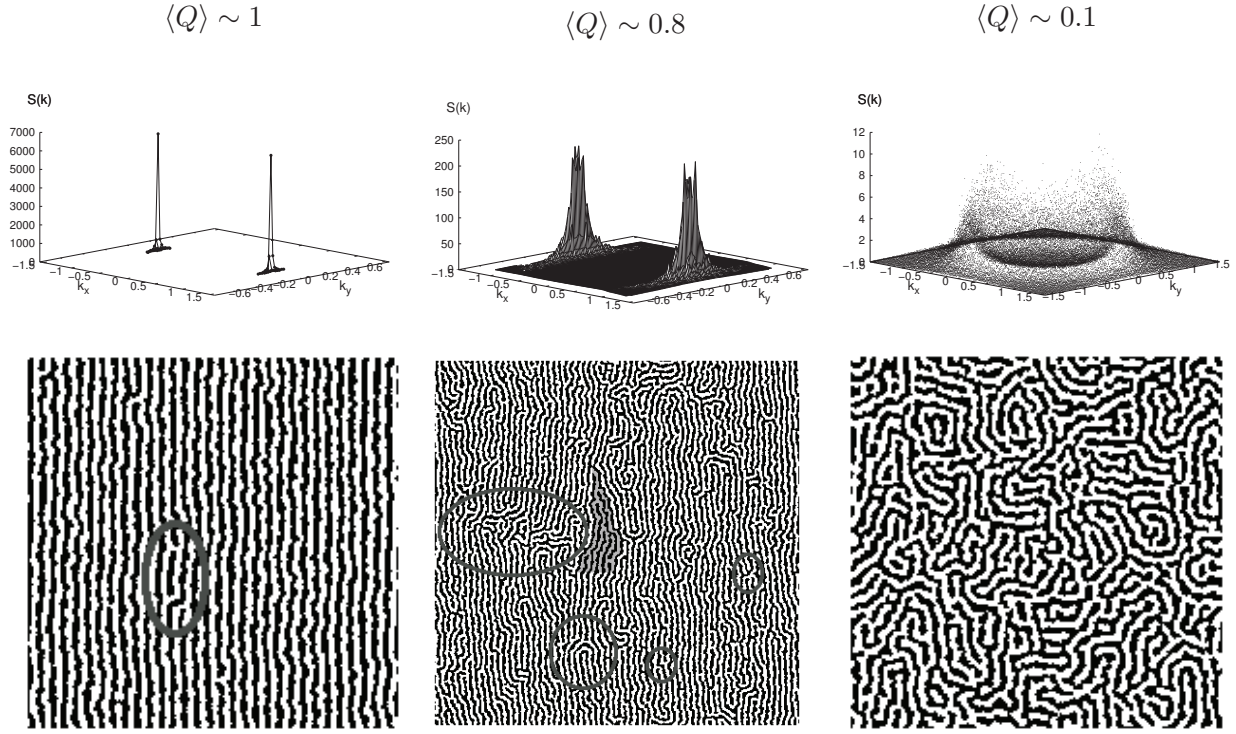

Figure 3. Results from Langevin simulations of the dipolar model at three temperatures, increasing from left to right. The stripe width span three lattice sites. Here are shown some representative configurations with sizes 192^2 (384^2 middle) with some topological defects highlighted, structure factors and mean orientational order parameter values corresponding to smectic, nematic and isotropic phases, respectively. Taken from [23].

but there is no periodicity under spatial translations. The nature of the nematic-isotropic phase transition was predicted to be of the Kosterlitz-Thouless type based on physically motivated arguments [24] and Langevin simulations on the dipolar case [23] gave support on this finding, in spite of some limitations due to numerical lattice induced anisotropies. Some results from this Langevin simulations, shown in Figure 3, are particularly relevant to illustrate the nematic order and its associated order parameter and angle fluctuations in the structure factor.

The recent introduction of a new elastic theory allowed us to identify the degrees of freedom at the relevant (wavelength) scale and to make precise analytical predictions on the nature of phase transitions in stripe forming systems in two dimensions, for arbitrary values of the range of the competing interaction $1/r^\alpha$ [1]. Allowing for the phase of the modulation to fluctuate in a way that the local order parameter is given by $\phi(\vec{x}) = \sum_n \phi_n \cos(nk_0 x + nk_0 u(\vec{x}))$, the effective Hamiltonian for the deformation field $u(\vec{x})$ has the following form:

$$\mathcal{H}_p = \frac{1}{2}\int \frac{d^2k}{(2\pi)^2}(\gamma_x k_x^2 + \gamma_y k_y^4 + \gamma_{nl} k^{\alpha-2} {k_y}^4)\hat{u}(\vec{k})\hat{u}(-\vec{k}). \quad (2)$$

The first two contributions of this effective Hamiltonian correspond to the well known local elastic response of the stripe pattern [25], while the last contribution is related with the residual interaction between the stripes due to the presence of a long range repulsive interaction of the form $1/r^{\alpha}$ [1]. It is possible to verify that for repulsive interactions sufficiently long-ranged ($\alpha < 2$), the non-local contribution in the effective Hamiltonian (2) dominates over the transversal local contribution. This is an unexplored regime in the literature, since previous works always assumed that even in the presence of long-range interactions the effective Hamiltonian possess only local contributions.

Nevertheless, a careful analysis of the positional fluctuations at a Gaussian level reveals that $\langle u^2 \rangle$ diverges linearly with the linear dimension of the system for $\sigma \geq 2$ and with a power $\frac{\sigma}{2}$ for $\sigma < 2$. This means that, independently of the range of the interaction, positional order is unstable.

On the other hand, it was proven that at scales much larger than the modulation length the effective orientational Hamiltonian in terms of the normalised local average of the director field $\vec{n}(\vec{x})$ is given by:

$$\begin{aligned} \mathcal{H}_o &= \frac{\gamma_1}{2} \int d^2x \, (\partial_\mu \vec{n}(\vec{x}))^2 + \frac{\gamma}{2} \int d^2x \int d^2x' \Omega(|\vec{x} - \vec{x}'|) \left(\frac{\vec{n}(\vec{x}) \cdot \vec{n}(\vec{x}')}{|\vec{x} - \vec{x}'|^{\sigma+2}} \right. \\ &- \left. (\sigma + 2)(\frac{\vec{n}(\vec{x}) \cdot (\vec{x} - \vec{x}') \vec{n}(\vec{x}') \cdot (\vec{x} - \vec{x}')}{|\vec{x} - \vec{x}'|^{\sigma+4}} \right), \end{aligned} \tag{3}$$

where γ_1 and γ represent the local and the non-local stiffnesses, respectively, and $\Omega(x)$ represents a short distance cut-off function. This Hamiltonian has been previously studied by Maier et.al. [26] for the case $\sigma = 1$. As pointed out by their results, the anisotropic term of the non-local dipolar interaction is irrelevant for the critical properties in two dimensions. This simplifies greatly the study to be made, since it makes it possible to replace the original non-local interaction by a ferromagnetic one decaying with the same power-law of that in the original orientational Hamiltonian without changing the critical properties of the model.

With this considerations in mind, it is straightforward to conclude that in systems with sufficiently long-ranged interactions ($\sigma < 2$) the non-local attractive interaction rules over the local contribution, stabilising a long-range orientational order at low temperatures. On the other hand, when $\sigma \geq 2$, the short ranged square gradient interaction dominates over the non-local contribution, resulting in the known Kosterlitz-Thouless (KT) transition scenario of the classical XY model [25].

For the new interesting case with $\sigma < 2$, the critical properties have been worked out by non-perturbative renormalization group techniques, and can be summarised as:

(i) in the critical region the correlation length diverges exponentially at T_c from both sides, as a reminiscent of the KT transition behaviour:

$$\xi_o \propto \exp\left(\frac{b}{\sqrt{|T_c - T|}} \right), \tag{4}$$

(ii) For $T < T_c$ in the critical region, the average order parameter behaves as $M \propto \xi_o(T)^{-(2-\alpha)/2}$, showing the existence of long-range order when $\alpha < 2$.

(iii) The orientational susceptibility diverges as $\chi_o \propto \xi_o(T)^{\alpha}$ in the critical region.

In the following section we present some of the main difficulties in exploring these and other features of two dimensional rotational symmetry breaking systems in numerical simulations. After a brief review of previous results about the nematic phase in the dipolar case, we present our method and recent results confirming the above scenario.

3. Simulations

In order to explore further this rich phenomenology in the complementary perspective of statistical physics simulations, it is important to have the proper tools for the phenomenon of interest. A traditional approach is to perform Monte Carlo simulations of the corresponding Ising model: $H = -\delta \sum_{<i,j>} s_i s_j + \sum_{(i,j)} s_i s_j / r_{ij}^{\alpha}$ [27, 28]. Even though this methodology is very useful to explore many interesting and general thermodynamic [29] and dynamical [30, 31] phenomena present in these stripe forming systems, their "microscopic" approach is affected by strong lattice effects. This lattice anisotropy is the result of the sharp (Ising) domain walls between each stripe in combination with the relative small stripe width (typically from 2 to 4 spins per stripe). In this conditions the system is dominated by the square lattice discrete symmetry, such that at high temperatures the disordered stripes form what is commonly called a tetragonal liquid [32]. The strong lattice induced anisotropy present in such simulations naturally prevent the study of rotational symmetry breaking phenomena of a priori isotropic models.

Instead, we take as starting point the same mesoscopic coarse-grained model (1), that can be seen as the effective, long wavelength limit of the corresponding Ising models. Simulations of field theory models such as these have been made extensively in the past, with Monte Carlo [33, 34], Langevin dynamics [35], or a combination of the two [36]. We have built on the methodology developed for the study of phase-ordering kinetics [37, 38, 39] and general dynamical critical phenomena [40]. Besides the many interesting dynamic features of the out-of-equilibrium dynamics of the stripe forming systems - a comprehensive review can be found in [41] - the same machinery can be applied to study their thermodynamic equilibrium properties.

Early studies of the nematic phase from Langevin simulations of the dipolar model revealed important large-scale features of a nematic phase, like anisotropic domains (shorter in the direction parallel to the stripes) and angle fluctuations (see the structure factor in Figure 3). On the other hand we observed long-range correlations in the nematic order instead of the expected quasi-long range order: fourfold lattice anisotropies, though softened because of the continuous nature of the order parameter field, were induced mainly by the short stripe width, of only three lattice sites per stripe. The effect of the four-fold anisotropy was to disrupt the orientational Goldstone excitation and changing the associated KT transition into a second-order phase transition [42, 43]. As it will become evident below, wider stripes are much less susceptible to such anisotropies at moderate temperatures. We now proceed to present the technical details of the Langevin simulations developed for this work.

3.1. Method

We performed Langevin simulations of the Hamiltonian (1). The relaxational (overdamped) Langevin dynamics of the density $\phi(\vec{x})$ is defined by:

$$\frac{\partial \phi(\vec{x})}{\partial t} = -\frac{\delta H[\phi]}{\delta \phi(\vec{x})} + \eta(\vec{x}, t), \tag{5}$$

which for the Hamiltonian in (1) reads:

$$\frac{\partial \phi}{\partial t}(\vec{x}, t) = \nabla^2 \phi - \frac{1}{\delta} \int d^2x' \frac{1}{|\vec{x} - \vec{x}'|^{\alpha}} \phi(\vec{x}', t) + r\phi(\vec{x}, t) - u\phi(\vec{x}, t)^3 + \eta(\vec{x}, t) \tag{6}$$

where δ and u are fixed parameters, $r = (T_c - T)$ and $\eta(\vec{x})$ represents a Gaussian white noise with correlations $\langle \eta(\vec{x}, t)\eta(\vec{x}', t') \rangle = 2T\delta(\vec{x} - \vec{x}')\delta(t - t')$, where T is the effective temperature of

the heat bath. In the Fourier space, this equation reads:

$$\frac{\partial \phi}{\partial t}(\vec{k},t) = -\mathcal{A}_\alpha(k)\phi(\vec{k},t) - u\left[\phi^3\right]_F(\vec{k},t) + \eta(\vec{k},t) \tag{7}$$

where $\left[\phi^3\right]_F(\vec{k},t)$ stands for the Fourier transform of $\phi^3(\vec{x},t)$, and $\mathcal{A}_\alpha(k)$ encompasses both the short k^2 and long-range $\mathcal{J}_\alpha(k)$ interactions. We worked with two forms of this kernel, the first

$$\mathcal{A}_3(k) = a_2(k-k_0)^2 - r \tag{8}$$

corresponds to the functional form of a dipolar interaction, basically from the linear dependence[44] in k. The second form is

$$\mathcal{A}_1(k) = a_2(k^2 + 2k_0^3/k - 3k_0^2) - r, \tag{9}$$

corresponding to the Coulomb model $1/k$. The parameters are such that both models have the same value of $\mathcal{A}_\alpha(k)$ and curvature close to the minimum k_0. To ensure this, we have set $a_2 = 1$ for the dipolar and $a_2 = 1/3$ for the Coulomb model. In both cases $T_c = 1$ and $k_0 = 1$.

The general solution of equation (7) is:

$$\phi(t+dt,\vec{k}) = \phi(t,\vec{k})\,\mathrm{e}^{-\mathcal{A}_\alpha(k)\,dt} + \int_t^{t+dt}\left[-u\left[\phi^3\right]_F(\vec{k},t') + \eta(\vec{k},t')\right]\mathrm{e}^{-\mathcal{A}_\alpha(k)\,(t+dt-t')}dt' \tag{10}$$

The general assumption towards the numerical integration of this equation is to consider the nonlinear part to be nearly constant during the time-step, between t and $t+dt$. The same cannot be assumed for the noise. By the central limit theorem, this integral is another Gaussian white noise with zero mean and variance such that, the general solution can be written as:

$$\phi(t+dt,\vec{k}) \simeq \phi(t,\vec{k})\,\mathrm{e}^{-\mathcal{A}_\alpha(k)\,dt} - u\left[\frac{1-\mathrm{e}^{-\mathcal{A}_\alpha(k)\,dt}}{\mathcal{A}_\alpha(k)}\right]\left[\phi^3\right]_F(\vec{k},t) + \sqrt{\frac{1-\mathrm{e}^{-2\mathcal{A}_\alpha(k)\,dt}}{2\mathcal{A}_\alpha(k)}}\,\mu(\vec{k}) \tag{11}$$

where $\mu(\vec{k})$ is the same Gaussian white noise integrated in time: $\langle\mu(\vec{x})\mu(\vec{x}')\rangle = 2T\delta(\vec{x}-\vec{x}')$. Since we are dealing with a system with many degrees of freedom, we always seek for simple methods of order one to minimize the computational cost.

3.2. Dipolar case

The Euler scheme can be obtained expanding to first order in dt so that:

$$\phi(t+dt,\vec{k}) \simeq \phi(t,\vec{k})\,[1-\mathcal{A}_\alpha(k)\,dt] - dt\,u\,\left[\phi^3\right]_F(\vec{k},t) + \sqrt{dt}\,\mu(\vec{k}) \tag{12}$$

where it was taken into account the same approximation to the variance of the noise. The stability of this method is very poor [45]. A typical treatment to enhance the stability is to implement it as a semi-implicit scheme, where the laplacian term from (8) is computed in $t+dt$:

$$(1+dt\,k^2)\phi(t+dt,\vec{k}) = \phi(t,\vec{k})\,[1+r\,dt-dt\,2k-dt] + \left[-dt\,u\,\phi^3(\vec{x},t) + \sqrt{dt}\,\mu(\vec{x})\right]_F(\vec{k},t) \tag{13}$$

where we have taken $k_0 = a_2 = 1$ as mentioned before, and have explicitly written the Fourier transform of the white noise. This is very close to the final implementation, we only have to address the spatial discretization. In the adimensional form where $k/k_0 \to k$ [41], the periodicity of the stripes are set by the lattice constant dx of the 2D square grid with linear size $L = MN$,

so that $\vec{k} = (k_x, k_y)$ with $k_i = 2\pi n_i/(dx\,L)$, $n_i = -L/2, \ldots, L/2$ and $dx = \pi/M$. Within this scheme, the stripe length span M lattice sites and the linear system size is such that contains N stripes. Then, full lattice update is accomplished in the Fourier space, with the aid of fast Fourier libraries [46] through:

$$\phi(t+dt,\vec{k}) = \frac{1 + r\,dt - dt\,2k - dt}{1 + dt\,k^2}\phi(t,\vec{k}) + \frac{1}{1+dt\,k^2}\left[-dt\,u\,\phi^3(\vec{x},t) + \sqrt{\frac{2T\,dt}{dx^2}}\,\tilde{\mu}\right]_F(\vec{k},t) \quad (14)$$

where $\tilde{\mu}$ is a Gaussian white noise with zero mean and unitary variance (in the discretization process Dirac deltas turn into Kronecker deltas: $\delta(\vec{x}-\vec{x}') \to \delta_{\vec{x},\vec{x}'}/dx^2$). Note that this scheme can be written in the form:

$$\phi(t+dt,\vec{k}) = \mathcal{L}(k)\phi(t,\vec{k}) + \mathcal{I}(k)\psi(t,\vec{k}) \quad (15)$$

where the real coeficients can be calculated at the start of the program $\mathcal{L}(k) \equiv (1 + r\,dt - dt\,2k - dt)/(1 + dt\,k^2)$, $\mathcal{I}(k) \equiv 1/(1+dt\,k^2)$ and $\psi(t,\vec{k}) \equiv \left[-dt\,u\,\phi^3(\vec{x},t) + \sqrt{2T dt/dx^2}\,\tilde{\mu}\right]_F$. This way the computational performance is dominated by the two forward FFT, L^2 updates and then one backward FFT. The main advantages of updating in the Fourier space are the decoupling of the equations (memory speedup) as well as the use of an isotropic form for the laplacian, minimizing one possible source of undesired lattice effects.

3.3. Coulomb case

One can readily see that, in the Coulomb case where the fluctuation spectrum (9) has one term inversely proportional to k, we would have $\phi(t+dt,\vec{k}) \propto \phi(t,\vec{k})/k$ and there would be an instability close to $k \sim 0$ that cannot be attenuated by any implicit term in an Euler scheme. Instead, we take advantage of the general solution given by (10) where $\phi(t+dt,\vec{k}) \propto \phi(t,\vec{k})\exp(-1/k)$ and this instability can be exponentially attenuated. In order to write the equation (11) in a simple form as in equation (15), we can see that we have know two different coefficients for the non-linear part:

$$\mathcal{I}_1(k) \equiv \left[\frac{1 - \mathrm{e}^{-\mathcal{A}_1(k)\,dt}}{\mathcal{A}_1(k)}\right] \quad \text{and} \quad \mathcal{I}_2(k) \equiv \sqrt{\frac{1 - \mathrm{e}^{-2\mathcal{A}_1(k)\,dt}}{2\mathcal{A}_1(k)}} \quad (16)$$

for the contributions of the ϕ^3 and the μ terms, respectively. We can notice that both this terms are similar for small dt, especially if we write them in power series: $\mathcal{I}_1(k) \simeq dt - \mathcal{A}_1(k)dt^2/2 + \mathcal{A}_1^2(k)dt^3/6 + \ldots$, and $\mathcal{I}_2(k) \simeq dt^{1/2} - \mathcal{A}_1(k)dt^{3/2}/2 + \mathcal{A}_1^2(k)dt^{5/2}/4.8 + \ldots$, so that up to second order in dt we can assume $\mathcal{I}_2(k) \simeq \mathcal{I}_1(k)/\sqrt{dt}$. Using this approximation for the coefficient of the thermal noise we have the same update form as in equation (15), with:

$$\mathcal{L}(k) \equiv \mathrm{e}^{-\mathcal{A}_1(k)\,dt} \quad (17)$$

$$\mathcal{I}(k) \equiv \frac{1 - \mathrm{e}^{-\mathcal{A}_1(k)\,dt}}{\mathcal{A}_1(k)} \quad (18)$$

$$\psi(t,\vec{k}) \equiv \left[-dt\,u\,\phi^3(\vec{x},t) + \sqrt{\frac{2T}{dt\,dx^2}}\,\tilde{\mu}\right]_F \quad (19)$$

3.4. Simulation results

With suitable stable schemes for the integration of the equations, the next step it to ensure an suitable space discretization to explore the properties of the nematic phases. By exploring the temperature range with cooling protocols with small system size, we could estimate the liquid-nematic phase transition. After an estimation of the equilibration and correlation times from high temperature quench experiments, we could safely guarantee that below $T \simeq 0.59$ ($T \simeq 0.44$) the configurations find themselves in the low temperature phase (with orientational order) for all system sizes for the dipolar (Coulomb) model. Within this low temperature phase but still in the neighbourhood of the phase transition, we have measured the structure factor for various thermal histories and different stripe widths M, related to space discretization by $dx = \pi/M$, from $M = 3$ up to $M = 15$. We have obtained an isotropic average structure factor for $M > 7$, meaning the stripes don't have a preferred direction in the nematic phase, so that lattice anisotropies are irrelevant. A conservative choice along this work was $M = 11$ in order to assure smooth domain walls.

Since above the aforementioned temperatures the configurations are in the stripe-liquid phase, where both positional and orientational correlation lengths are finite, we have concentrated our efforts on equilibrium simulations inside the nematic phase, with $T = 0.57$ ($T = 0.43$) for the dipolar (Coulomb) model, for system sizes ranging from $(12 \times 11)^2$ up to $(66 \times 11)^2$.

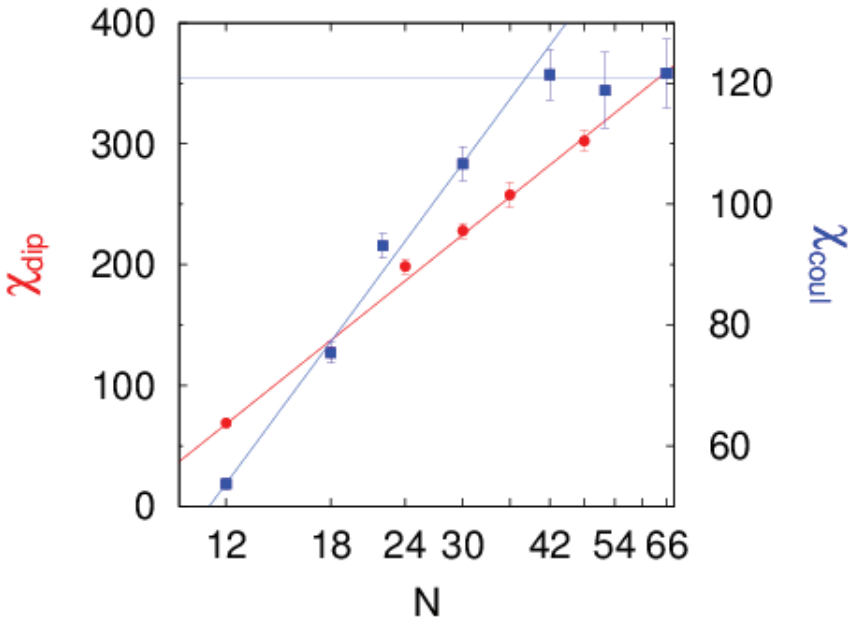

Figure 4. Orientational susceptibility in linear-log scale plot of the Coulomb (right) and dipolar (left) models as function of the linear size of the systems (normalized by half of the modulation length N=L/11). The full lines are fits to logarithmic function $A + B \log N$, with: $A = -355(18)$ and $B = 170(6)$ ($\chi^2/N_{dof} = 1.0$) in the dipolar case; $A = -362(10)$ and $B = 173(4)$ ($\chi^2/N_{dof} = 2.3$) in the Coulomb case. In both cases the number of degrees of freedom is $N_{dof} = 3$. The horizontal line is only a guide to the eyes.

In order to quantify the orientational order, through the local director field $\vec{n}(\vec{x}) =$

$\vec{\nabla}\phi(\vec{x})/|\vec{\nabla}\phi(\vec{x})|$ we have measured the nematic tensor:

$$Q_{\alpha\beta} = \sum_{\vec{x}} \left(n_a(\vec{x}) n_a(\vec{x}) - \frac{1}{2}\,\delta_{\alpha\beta} \right) \tag{20}$$

where $\alpha, \beta = 1, 2$ are the Cartesian components. The orientational order parameter is given by $Q = \sqrt{Q_{11}^2 + Q_{12}^2}$. We have measured this quantity and its corresponding susceptibility χ using between 5 and 25 thermal histories, resulting approximately in an overall $2 \times 10^6/N^2$ ($3 \times 10^6/N^2$) independent measurements for the dipolar (Coulomb) model - recalling that N is the number of stripes that can fit in the linear size of the system, both related by $N = L/11$, so the number of samples lies roughly between 700 and 20000.

Our results are shown in Figures 4 and 5. We can readily see from Figure 4 that below the transition temperature the susceptibility of the corresponding order parameter presents a limited growth up to a plateau for the Coulomb case. This is what is expected in a second order phase transition. On the other hand, with dipolar interactions we observe a monotonic (probably logarithmic) increase of the susceptibility with the system size, without any sign of attenuation. This is in accordance with a Kosterlitz-Thouless phase, where the susceptibility should diverge in the thermodynamic limit for all $T \leq T_{KT}$. Even though we show logarithmic fits along the points in Figure 4, the small number of points don't allow to clearly distinguish this functionality from power-laws, algebraic fits are equally good [1] specially for the Coulomb case.

Of course, this is an analysis for a single low temperature and it presents a limited power if compared to more traditional finite-size scaling analysis. Indeed, we cannot conclude that the dipolar χ will not saturate at larger N's, but the different trend observed in both systems for equivalent parameter values is a strong indication that the theoretical results are indeed correct. In Figure 5 the value of the orientational order parameter as function of the linear size for both models are similar in behaviour, showing how subtle the characterization of both models can be.

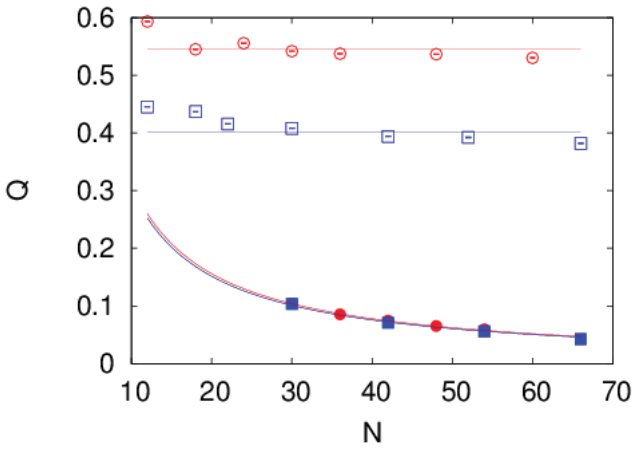

Figure 5. Orientational order parameter dependence on the normalized linear size of the systems for the Coulomb (blue) and dipolar (red) models, for temperatures above (filled) and below Tc (open symbols). These temperatures correspond to $T = 0.60$ ($T = 0.45$) and $T = 0.57$ ($T = 0.43$) for the dipolar (Coulomb) model. Horizontal lines are guides to the eyes, while the others are fits to A/N - with $A \sim 3$, a characteristic dependence on linear size of order parameter in the disordered phase.

4. Conclusions and perspectives

We found special difficulty equilibrating large systems at low temperatures, due to the high degree of degeneracy and frustration of these models - notorious to present slow and arrested dynamics [41, 47, 48]. A first step towards a speed up in computational time would be to implement an extended ensemble Langevin dynamics, like parallel tempering for example. To further explore the properties of the nematic phases, it is important to measure the nematic correlation functions, as done in previous work [23]. In this sense, it is important to notice that the current estimation of the local director field makes use of a second order finite-difference scheme to calculate the gradient. This makes the director field susceptible to local fluctuations, and working with higher order stencils doesn't make significant improvement. As such, the correlations fall off substantially in the short scales, making the quantification of long-range properties difficult to analyse. The approach taken previously was to smooth out fluctuation by filters. In order not to damage the local orientational information of the configuration, there are specially designed filters that conserve the directional properties of the stripes [49]. Another interesting approach is to estimate the director field with the aid of the gradient-square tensor in Fourier space [50]. Finally, we emphasize the positive general features of the Langevin simulation technique to study such pattern forming systems where isotropy is guaranteed by careful designed conditions (see Figure 6).

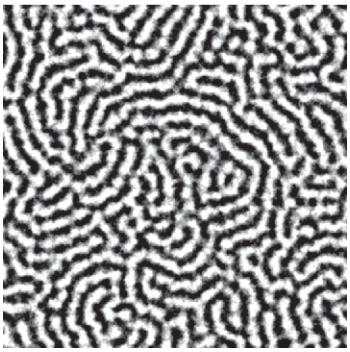

Figure 6. A typical $(42 \times 11)^2$ configuration of the isotropic phase for the dipolar model, close to the phase transition at $T = 0.60$.

We have presented results confirming the effect of the range of the competing isotropic interactions at the nature of the purely orientational low-temperature stripe phase, the nematic phase. In the dipolar interaction case orientational order parameter susceptibility seems to be divergent in the low temperature phase, characteristic of a critical phase as in the KT transition of XY model. Conversely, in the Coulomb interaction case we observed a saturation of this susceptibility, intrinsic to the broken symmetry phases of second order phase transitions. The similar behaviour for both cases close to the phase transition is in accordance with the reminiscent KT behaviour in equation (4). We expect to further explore the finite size properties of this distinctive behaviour in future extended simulations.

Acknowledgements
We gratefully acknowledge partial financial support from CNPq (Brazil) and the *Laboratório de Física Computacional* from IF-UFRGS for the utilization of the cluster Ada.

References

[1] Mendoza-Coto A, Stariolo D A and Nicolao L 2015 *Phys. Rev. Lett.* **114**(11) 116101

[2] Fischer K H and Hertz J A 1991 *Spin Glasses* (Cambridge: Cambridge University Press)
[3] Hubert A and Schafer R 1998 *Magnetic Domains* (Berlin: Springer-Verlag)
[4] Vega D A, Harrison C K, Angelescu D E, Trawick M L, Huse D A, Chaikin P M and Register R A 2005 *Phys. Rev. E* **71** 061803
[5] Kivelson S A, Fradkin E and Emery V J 1998 *Nature* **393** 550
[6] Vaterlaus A, Stamm C, Maier U, Pini M G, Politi P and Pescia D 2000 *Phys. Rev. Lett.* **84** 2247–2250
[7] Brazovskii S A 1975 *Sov. Phys. JETP* **41** 85–89
[8] Swift J and Hohenberg P C 1977 *Physical Review A* **15** 319
[9] Emery V and Kivelson S 1993 *Physica C: Superconductivity* **209** 597 – 621 ISSN 0921-4534
[10] Fradkin E and Kivelson S A 1999 *Phys. Rev. B* **59** 8065–8072
[11] Fradkin E, Kivelson S A, Lawler M J, Eisenstein J P and Mackenzie A P 2010 *Annual Review of Condensed Matter Physics* **1** 153–178
[12] Kivelson S A, Bindloss I P, Fradkin E, Oganesyan V, Tranquada J M, Kapitulnik A and Howald C 2003 *Rev. Mod. Phys.* **75**(4) 1201–1241
[13] Vojta M 2009 *Advances in Physics* **58** 699–820
[14] Fradkin E, Kivelson S A and Tranquada J M 2015 *Rev. Mod. Phys.* **87**(2) 457–482
[15] Strandburg K J 1988 *Rev. Mod. Phys* **60** 161–206
[16] Seul M and Andelman D 1995 *Science* **267** 476–483
[17] Wu Y Z, Won C, Scholl A, Doran A, Zhao H W, Jin X F and Qiu Z Q 2004 *Physical Review Letters* **93** 117205
[18] Abu-Libdeh N and Venus D 2009 *Phys. Rev. B* **80** 184412
[19] HAN J, WANG Q H and LEE D H 2001 *International Journal of Modern Physics B* **15** 1117–1126
[20] Borzi R A, Grigera S A, Farrell J, Perry R S, Lister S J S, Lee S L, Tennant D A, Maeno Y and Mackenzie A P 2007 *Science* **315** 214–217
[21] Parker C V, Aynajian P, da Silva Neto E H, Pushp A, Ono S, Wen J, Xu Z, Gu G and Yazdani A 2010 *Nature* **468** 677–680
[22] Barci D G and Stariolo D A 2007 *Physical Review Letters* **98** 200604
[23] Nicolao L and Stariolo D A 2007 *Phys. Rev. B* . **76** 054453
[24] Barci D G and Stariolo D A 2009 *Physical Review B* **79** 075437
[25] Toner J and Nelson D R 1981 *Phys. Rev. B* **23** 316–334
[26] Maier P G and Schwabl F 2004 *Phys. Rev. B* **70**(13) 134430
[27] Löw U, Emery V J, Fabricius K and Kivelson S A 1994 *Phys. Rev. Lett.* **72**(12) 1918–1921
[28] MacIsaac A B, Whitehead J P, Robinson M C and De'Bell K 1995 *Phys. Rev. B* **51** 16033
[29] Cannas S A, Michelon M F, Stariolo D A and Tamarit F A 2006 *Phys. Rev. B* **73** 184425
[30] Cannas S A, Michelon M F, Stariolo D A and Tamarit F A 2008 *Phys. Rev. E* **78** 051602
[31] Gleiser P M, Tamarit F A, Cannas S A and Montemurro M A 2003 *Phys. Rev. B* **68** 134401
[32] Abanov A, Kalatsky V, Pokrovsky V L and Saslow W M 1995 *Phys. Rev. B* **51** 1023–1038
[33] Cooper F, Freedman B and Preston D 1982 *Nuclear Physics B* **210** 210 – 228 ISSN 0550-3213
[34] Milchev A, Heermann D and Binder K 1986 *Journal of Statistical Physics* **44** 749–784 ISSN 0022-4715
[35] Davies C, Batrouni G, Katz G, Kronfeld A, Lepage P, Rossi P, Svetitsky B and Wilson K 1986 *Journal of Statistical Physics* **43** 1073–1075 ISSN 0022-4715
[36] Ukawa A 2015 *Journal of Statistical Physics* **160** 1081–1124 ISSN 0022-4715
[37] Langer J S, Bar-on M and Miller H D 1975 *Phys. Rev. A* **11**(4) 1417–1429
[38] Bray A J 1994 *Advances in Physics* **43** 357
[39] Roland C and Desai R 1990 *Phys. Rev. B* **42** 6658
[40] Hohenberg P C and Halperin B I 1977 *Rev. Mod. Phys.* **49** 435–479
[41] Daz-Mndez R, Mendoza-Coto A, Mulet R, Nicolao L and Stariolo D 2011 *The European Physical Journal B* **81**(3) 309–319 ISSN 1434-6028
[42] José J V, Kadanoff L P, Kirkpatrick S and Nelson D R 1977 *Phys. Rev. B* **16**(3) 1217–1241
[43] Taroni A, Bramwell S T and Holdsworth P C W 2008 *Journal of Physics: Condensed Matter* **20** 275233
[44] Jagla E A 2004 *Phys. Rev. E* **70** 046204
[45] Vollmayr-Lee B P and Rutenberg A D 2003 *Phys. Rev. E* **68**(6) 066703
[46] Frigo M and Johnson S 2005 *Proceedings of the IEEE* **93** 216–231 ISSN 0018-9219
[47] Ribeiro Teixeira A C, Stariolo D A and Barci D G 2013 *Phys. Rev. E* **87**(6) 062121
[48] Riesch C, Radons G and Magerle R 2014 *Phys. Rev. E* **90**(5) 052101
[49] Harrison C, Cheng Z, Sethuraman S, Huse D A, Chaikin P M, Vega D A, Sebastian J M, Register R A and Adamson D H 2002 *Phys. Rev. E* **66**(1) 011706
[50] van de Weijer J, van Vliet L, Verbeek P and van Ginkel R 2001 *Pattern Analysis and Machine Intelligence, IEEE Transactions on* **23** 1035–1042 ISSN 0162-8828